

Next-to-leading order QCD corrections to $\chi_{cJ}W^+b$ associated production from top-quark decay

Zhou Chao¹, Li Gang^{1,*}, Song Mao¹, Ma Wen-Gan², and Zhang Ren-You²

¹ *School of Physics and Materials Science, Anhui University,
Hefei, Anhui 230039, People's Republic of China and*

² *Department of Modern Physics, University of Science and Technology of China (USTC),
Hefei, Anhui 230026, People's Republic of China*

(Dated: December 16, 2016)

Abstract

We calculate the next-to-leading order QCD corrections to the excited charmonium χ_{cJ} associated with W^+b production from top-quark decay. Our results show that detecting the χ_{c0} production from top-quark decay is very difficult, but the χ_{c1} and χ_{c2} productions have the potential to be detected at the LHC. If the prompt χ_{cJ} production from top-quark decay is really detected at the LHC, it will be useful not only for investigating J/ψ production from top-quark decay but also for understanding the heavy quarkonium production mechanism.

PACS numbers: 12.38.Bx, 14.40.Pq, 14.65.Ha

*Electronic address: lig2008@mail.ustc.edu.cn

I. INTRODUCTION

Heavy quarkonium is a multiscale system, which offers a good testing ground for investigating the QCD in both perturbative and nonperturbative regimes. The factorization formalism of nonrelativistic QCD (NRQCD) [1] as a rigorous theoretical framework to describe the heavy quarkonium production and decay has been widely investigated both in experimental and theoretical aspects. People believe that NRQCD, the only effective field theory allowing for consistent QCD-based calculations beyond the Born approximation, may be the most promising theory to describe the heavy quarkonium physics.

Through efforts from both the experimental and theoretical sides, substantial progress has been achieved in heavy quarkonium physics, many processes have been calculated to next-to-leading order(NLO) in α_s [2–14]. For the prompt J/ψ production, almost all the relevant observable predictions are available at the NLO, and based on different philosophies, the color-octet(CO) long-distance matrix elements (LDMEs) of J/ψ have been extracted by three groups independently. It has been found that for quarkonium production and decay in the framework of NRQCD in many cases the leading order(LO) calculation is inadequate and the NLO QCD corrections are crucial. The discrepancies between LO calculations and unpolarized experimental results are fairly well described by the NRQCD theory through including higher order corrections[9, 15–18]. But for polarization production, though the NLO corrections have been considered, people are not able to fully explain the polarization production by theoretical analyses in a way consistent with the world data on the unpolarized yield, and the polarization puzzle still poses a challenge to the heavy quarkonium physics[19, 20].

Therefore, a further test the mechanism of quarkonium production is needed, and more processes of heavy quarkonium production and decay should be investigated. The study of the production for excited charmonium other than J/ψ may also be valuable, not only is the study of excited heavy quarkonium production important for J/ψ production for the excited heavy quarkonium to be able to radiatively decay to J/ψ , but also the study of excited heavy quarkonium production itself can directly deepen our understanding about QCD. Many processes of χ_{cJ} ($J = 0, 1, 2$) production at the Tevatron and LHC have been studied up to the NLO, and the $r = \frac{m_c^2 \langle \mathcal{O}^{\chi_{c0}}[{}^3S_1^{(8)}] \rangle}{\langle \mathcal{O}^{\chi_{c0}}[{}^3P_0^{(1)}] \rangle}$ has been given by using the Tevatron data, LHCb data and CMS data. But its accuracy is not very satisfying; the r value can be

varied from 0.21 to 0.35 in fitting different data with different hypotheses [7, 10].

At the LHC, The latest estimations for $\sigma(pp \rightarrow t\bar{t}X)$ range from 874_{-33}^{+14} pb [21] to $943 \pm 4(\text{kinematics})_{-49}^{+77}(\text{scale}) \pm 12(\text{PDF})$ pb [22] for $m_t = 173$ GeV and $\sqrt{s} = 14$ TeV. Therefore, it is significant to perform detailed study of heavy quarkonium production from top-quark decay at the LHC. Many heavy quarkonium productions from top-quark decay processes have been calculated at the LO[23–26], and the decay widths of top quark to S-wave $\bar{b}c$, $\bar{c}c$ and $\bar{b}b$ bound states at the NLO are available now[27, 28]. For the investigation of $t \rightarrow \chi_{cJ} + W^+ + b$ processes may provide important information not only for the J/ψ associated with W^+b production from top-quark decay but also can provide an excellent platform to extract the universality LDMEs of χ_{cJ} . In this paper, we will calculate the $t \rightarrow \chi_{cJ} + W^+ + b$ processes up to the NLO in α_s within the NRQCD framework by applying the covariant projection method[29]. The paper is organized as follows. in Sec.II, we present the details of the calculation strategies, and Sec.III is arranged to present the numerical results. Finally, a short summary and discussions are given.

II. CALCULATION DESCRIPTIONS

In this section, we present the calculation about the decay width for processes $t \rightarrow \chi_{cJ} + W^+ + b + X$ to the NLO of α_s . At the LO, only the $^3S_1^{(8)}$ Fock state has made a contribution, and the Feynman diagrams for this partonic process are drawn in Figs. 1(a) and 1(b). In the nonrelativistic limit, the short-distance coefficients of $^3S_1^{(8)}$ Fock state for processes $t \rightarrow \chi_{cJ} + W^+ + b + X$ are the same as the process $t \rightarrow J/\psi + W^+ + b + X$ in $^3S_1^{(8)}$ Fock state at the LO. Applying the covariant-projector method of Ref.[29], we can get analytic short-distance coefficients of processes $t \rightarrow \chi_{cJ} + W^+ + b + X$, which are the same as in Refs.[25, 28].

The NLO QCD corrections contain the virtual correction and the real gluon emission correction; the former is only related to $^3S_1^{(8)}$ Fock-state contribution, and the latter involves $^3S_1^{(8)}$ and $^3P_J^{(1)}$ Fock-state contributions. Some representative loop and real gluon emission Feynman diagrams for the $t \rightarrow \chi_{cJ} + W^+ + b + X$ decay processes at the NLO are presented in Figs. 1(c)-1(p). There exist UV, soft and coulomb singularities in virtual correction, and soft singularities will emerge from both the $^3S_1^{(8)}$ Fock-state and $^3P_J^{(1)}$ Fock-state contributions when we calculate the real gluon emission process. The UV divergences from the virtual

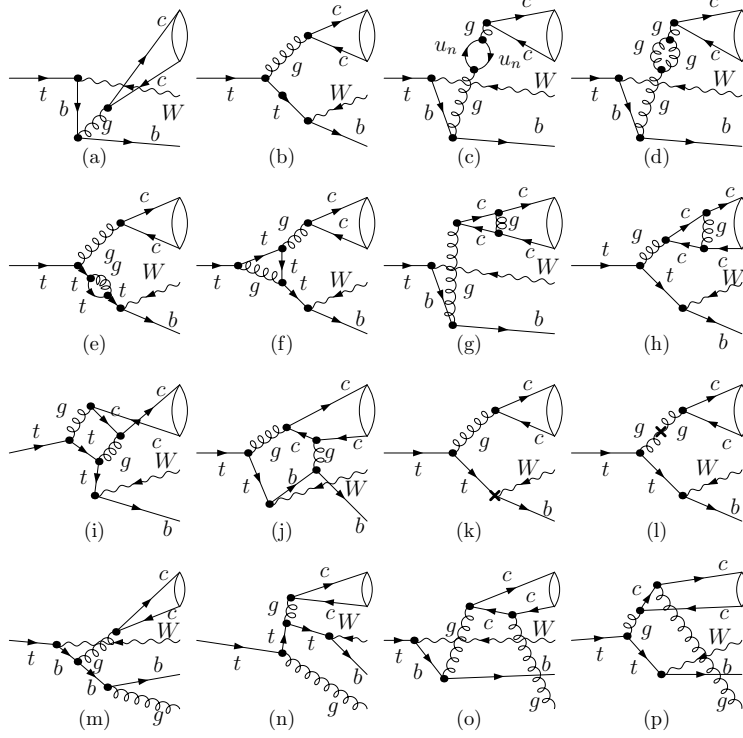


FIG. 1: Some representative LO and QCD NLO Feynman diagrams for the $t \rightarrow \chi_{cJ} + W^+ + b$ decay processes. Where (a) and (b) are tree level diagrams, (c)-(j) are part loop diagrams, (k)-(l) are part counterterms diagrams and (m)-(p) are part real gluon emission diagrams for $t \rightarrow \chi_{cJ} + W^+ + b$ decay process.

correction are removed after renormalization procedure. The soft divergences from the one-loop diagrams will be canceled by similar singularities from the ${}^3S_1^{(8)}$ Fock-state contribution of soft real gluon emission. Nevertheless, it still contains coulomb singularities in virtual correction and soft singularities arising from the ${}^3P_J^{(1)}$ Fock-state contribution of real gluon process. These singularities are not infrared divergence in the usual sense, and they can only be eliminated in the spirit of the factorization approach, by taking the corresponding corrections to the operator $\langle \mathcal{O}_{\chi_{cJ}}[{}^3S_1^{(8)}] \rangle$ into account. In Fig. 2, we present the divergence structure and divergence cancellation routes in the NLO calculation for the $t \rightarrow \chi_{cJ} + W^+ + b$.

In our calculations, the dimensional regularization scheme is adopted to regularize the UV and IR divergences under t'Hooft-Feynman gauge. We use the modified minimal subtraction ($\overline{\text{MS}}$) and on-mass-shell schemes to renormalize the strong coupling constant and the quark wave functions, respectively. A small relative velocity v between c and \bar{c} has been used to regularize coulomb singularities[30] for Fig. 1(g) and 1(h) in the virtual correction

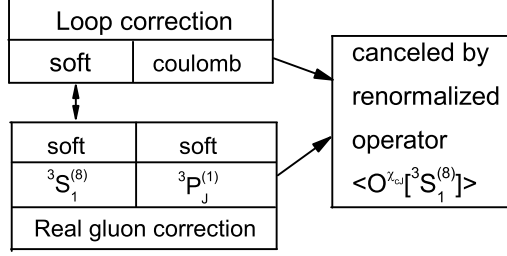


FIG. 2: The IR and Coulomb singularity structures in the NLO QCD calculations for the $t \rightarrow \chi_{cJ} + W^+ + b$ decay processes.

calculation. Meanwhile, the phase space slicing (PSS) method [31] has been employed for dealing with the soft singularities in real gluon emission corrections.

When we calculate the short-distance coefficients of $^3S_1^{(8)}$ Fock state in the virtual and real gluon emission contribution, we use the strategy same as in Ref.[28]. The detail for the calculations of $^3S_1^{(8)}$ Fock-state contributions is too tedious to be presented here for the sake of brevity. As for the $^3P_J^{(1)}$ Fock-state decay contributions to the real gluon emission processes $t \rightarrow \chi_{cJ} + W^+ + b + g$, we denote the decay processes as

$$t(p_1) \rightarrow \chi_{cJ}(p_2) + W^+(p_3) + b(p_4) + g(p_5), \quad (1)$$

and some of the Feynman diagrams for these partonic processes are presented in Fig. 1(o) and 1(p).

There are soft singularities arising from the real gluon processes with $^3P_J^{(1)}$ Fock state, which can be isolated by slicing the phase space into two different regions based on PSS method. By introducing a small cutoff δ_s , the phase space of $t \rightarrow \chi_{cJ} + W^+ + b + g$ is separated into two regions, according to whether the emitted gluon is soft, i.e., $E_5 < \delta_s m_t/2$, or hard, i.e., $E_5 \geq \delta_s m_t/2$. In our numerical calculations, when δ_s varies from 10^{-5} to about 10^{-4} , the $\Delta\Gamma_{soft_{3P_J^{(1)}}}$ and $\Delta\Gamma_{hard_{3P_J^{(1)}}}$ remain almost unchanged at the value of about 1.0% of the total width. In further calculations, we set $\delta_s = 1 \times 10^{-4}$. Then the decay width for the processes $t \rightarrow \chi_{cJ} + W^+ + b + g$ with the $^3P_J^{(1)}$ Fock state can be expressed as

$$\begin{aligned} \Delta\Gamma_{real_{3P_J^{(1)}}}(t \rightarrow \chi_{cJ} + W^+ + b + g) &= \Delta\Gamma_{soft_{3P_J^{(1)}}}(t \rightarrow \chi_{cJ} + W^+ + b + g) \\ &+ \Delta\Gamma_{hard_{3P_J^{(1)}}}(t \rightarrow \chi_{cJ} + W^+ + b + g). \end{aligned} \quad (2)$$

$\Delta\Gamma_{hard_{3P_J^{(1)}}}$ is finite and can be integrated in four dimensions by using the Monte Carlo

method. Using the method of Ref.[29], we can get the expression of $\Delta\Gamma_{soft_{3P_J^{(1)}}}$ as

$$\begin{aligned}\Delta\Gamma_{soft_{3P_J^{(1)}}} &= -\left(\frac{1}{\epsilon} - 2\ln\delta_s + \frac{1}{\beta}\ln\frac{1+\beta}{1-\beta}\right)\frac{4\alpha_s C_F}{3\pi m_c^2} \\ &\times \frac{\Gamma(1-\epsilon)}{\Gamma(1-2\epsilon)}\left(\frac{4\pi\mu_r^2}{\hat{s}}\right)^\epsilon <\mathcal{O}^{\chi_{cJ}}[{}^3P_J^{(1)}]> \\ &\times \frac{\Gamma_{LO}}{<\mathcal{O}^{\chi_{cJ}}[{}^3S_1^{(8)}]>} \end{aligned} \quad (3)$$

with $\beta = \sqrt{1 - 4m_c^2/E_2^2}$ and where E_2 is the energy of χ_{cJ} and $C_F = \frac{N_c^2-1}{2N_c} = \frac{4}{3}$, for quark colors $N_c = 3$.

When we deal with the renormalization of the color octet ${}^3S_1^{(8)}$ LDME, we adopt the same method as in Ref. [12].

$$\begin{aligned}<\mathcal{O}^{\chi_{cJ}}[{}^3S_1^{(8)}]>_{Born} = <\mathcal{O}^{\chi_{cJ}}[{}^3S_1^{(8)}]>_r(\mu_\Lambda) \left[1 - \left(C_F - \frac{C_A}{2}\right)\frac{\pi\alpha_s}{2v}\right] \\ &+ \frac{4\alpha_s}{3\pi m_c^2}\left(\frac{4\pi\mu_r^2}{\mu_\Lambda^2}\right)^\epsilon \exp(-\epsilon\gamma_E)\frac{1}{\epsilon} \\ &\times \sum_{J=0}^2 \left(C_F <\mathcal{O}^{\chi_{cJ}}[{}^3P_J^{(1)}]> + B_F <\mathcal{O}^{\chi_{cJ}}[{}^3P_J^{(8)}]>\right), \end{aligned} \quad (4)$$

where μ_r is the t'Hooft mass scale and $B_F = \frac{N_c^2-4}{4N_c} = \frac{5}{12}$. μ_Λ is the NRQCD scale, where $v = |\vec{p}_c - \vec{p}_{\bar{c}}|/m_c$, defined in the meson rest frame, and we use this small relative velocity between c and \bar{c} to regularize the Coulomb singularities. Using the strategy shown in Fig. 2, after taking into account the NRQCD NLO corrections to the operator $<\mathcal{O}^{\chi_{cJ}}[{}^3S_1^{(8)}]>$, all the IR and Coulomb singularities can be cancelled, and we can get the finite NLO QCD corrected total decay width for the processes $t \rightarrow \chi_{cJ} + W^+ + b$. Then, the $t \rightarrow \chi_{cJ} + W^+ + b$ total decay width including the NLO QCD corrections can be obtained by summing all the contribution parts:

$$\begin{aligned}\Gamma_{NLO} &= \Gamma({}^3S_1^{(8)}) + \Gamma({}^3P_J^{(1)}) \\ &= \Gamma_{LO}({}^3S_1^{(8)}) + \Delta\Gamma_{Virtual}({}^3S_1^{(8)}) + \Delta\Gamma_{Real}({}^3S_1^{(8)}) + \Delta\Gamma_{Real}({}^3P_J^{(1)}) \end{aligned} \quad (5)$$

III. NUMERICAL RESULTS AND DISCUSSION

In the numerical calculations, we use one-loop and two-loop running α_s in the LO and NLO calculations, respectively, which means $\alpha_s(M_Z) = 0.130$ and $\alpha_s(M_Z) = 0.118$ for

the LO and NLO calculations, respectively. The relevant quark masses and fine structure constant are taken as: $m_q = 0$ ($q = u, d, s$), $m_c = m_{\chi_{cJ}}/2 = 1.5 \text{ GeV}$, $m_W = 80.398 \text{ GeV}$, $m_b = 4.75 \text{ GeV}$, $m_t = 173 \text{ GeV}$ and $\alpha = 1/137.036$. The renormalization and NRQCD scales are chosen as $\mu_r = m_t$ and $\mu_\Lambda = m_c$, respectively.

Following the heavy-quark spin symmetry, the multiplicity relations of LDMEs

$$\begin{aligned} \langle \mathcal{O}^{\chi_{cJ}}[{}^3P_J^{(1)}] \rangle &= (2J+1) \langle \mathcal{O}^{\chi_{c0}}[{}^3P_0^{(1)}] \rangle, \\ \langle \mathcal{O}^{\chi_{cJ}}[{}^3S_1^{(8)}] \rangle &= (2J+1) \langle \mathcal{O}^{\chi_{c0}}[{}^3S_1^{(8)}] \rangle \end{aligned} \quad (6)$$

can be assumed satisfied [1]. The relation between the color-singlet (CS) matrix elements $\langle \mathcal{O}^{\chi_{c0}}[{}^3P_0^{(1)}] \rangle$ of χ_{c0} and the P-wave function at the origin can be written as the formula $\langle \mathcal{O}^{\chi_{c0}}[{}^3P_0^{(1)}] \rangle = \frac{3N_c}{2\pi} |R'_P(0)|^2$. In predicting the production cross sections, $|R'_P(0)|^2 = 0.075 \text{ GeV}^5$ from the potential model calculations [32] has been used in our calculation.

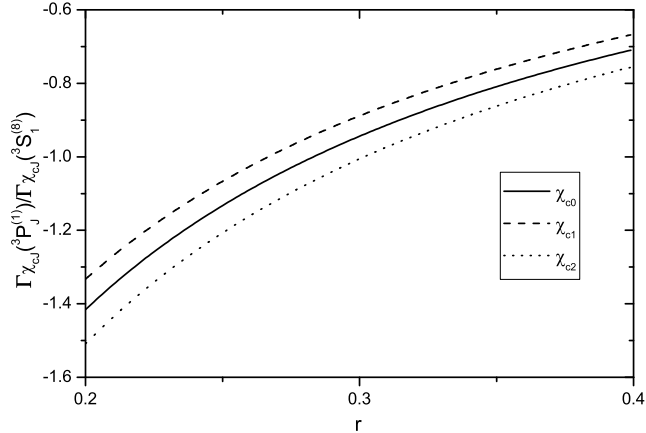


FIG. 3: The ratio of $\Gamma_{3P_J^{(1)}}$ to $\Gamma_{3S_1^{(8)}}$ at NLO as a function of the the matrix element ratio r for the processes $t \rightarrow \chi_{cJ} + W^+ + b$.

As for the CO matrix element $\langle \mathcal{O}^{\chi_{c0}}[{}^3S_1^{(8)}] \rangle$, though the NLO results have been obtained based on fitting the Tevatron data, LHCb data, and CMS data, its accuracy is very poor. The ratio $r = \frac{m_c^2 \langle \mathcal{O}^{\chi_{c0}}[{}^3S_1^{(8)}] \rangle}{\langle \mathcal{O}^{\chi_{c0}}[{}^3P_0^{(1)}] \rangle}$ is acceptable with $r = 0.27 \pm 0.06$ when fitting Tevatron data and CMS data. However, for the LHCb data, the value of r can be varied from 0.35 to 0.31 when using a different p_T cutoff. In Fig. 3, we present the ratio of $\Gamma_{3P_J^{(1)}}$ to $\Gamma_{3S_1^{(8)}}$ at the NLO as a function of the the matrix element ratio r for the processes $t \rightarrow \chi_{cJ} + W^+ + b$. In our calculations, we have not fixed the value of r and varied it from 0.20 to 0.40. From Fig.

3, we can see that the contribution from $^3P_J^{(1)}$ Fock state is very important and surprising with negative sign. This negative contribution of $^3P_J^{(1)}$ state is mainly due to the fact we have used the \overline{MS} subtraction scheme[7] in renormalizing the NRQCD LDMEs $\langle \mathcal{O}^{\chi_{cJ}}[{}^3S_1^{(8)}] \rangle$ and set factorization scale $\mu_\Lambda = m_c$. The $^3P_J^{(1)}$ Fock state contributions mainly come from the real gluon contribution and the operator contribution induced by the mixing of the $c\bar{c}$ Fock state NRQCD operators at one loop level [12], where the latter depends on the subtraction scheme and the factorization scale μ_Λ in the NLO calculation. But this dependence will be compensated by the corresponding one of the $^3S_1^{(8)}$ state contribution in the calculation of the total decay ratio $\Gamma_{\chi_{cJ}}$. From Eq(4), we can see that if we select a smaller μ_Λ it could even lead to a positive NLO P -wave contribution, but that scale may be too small, and the perturbative calculation will be unreliable. A physical quantity should be independent of the subtraction scheme and factorization scale if we perform all order calculation. But at finite order, the factorization scale dependence does not exactly cancel, leading to scale ambiguities. The dependence of the decay widths on the factorization scale μ_Λ induces important theoretical uncertainty. To estimate the theoretical uncertainties caused by the factorization scale, in Fig. 4, we present the μ_Λ dependence of the χ_{c0} NLO total decay width, the $^3S_1^{(8)}$ and $^3P_0^{(1)}$ channel decay widths. From Fig. 4, we can see that with the decrement of the value of μ_Λ the $^3P_0^{(1)}$ -channel state contribution increases slowly, and this increment of the $^3P_0^{(1)}$ -state contribution is partly compensated by the decrement of $^3S_1^{(8)}$ contribution. When the scale μ_Λ runs from 0.75 GeV to 3.0 GeV , the χ_{c0} NLO total decay width slightly increases with the rise of μ_Λ .

Top-quark decays within the Standard Model are dominated by the mode $t \rightarrow b + W^+$ for $V_{tb} = 1$. To get the branching ratio of the decay processes $t \rightarrow \chi_{cJ} + W^+ + b$, in our work, the Born approximation decay widths of processes $t \rightarrow b + W^+$ has been used[28]. As shown in Fig. 3, the bound of $r > 0.301$ is needed to gain a positive decay width for the process $t \rightarrow \chi_{cJ} + W^+ + b$. In Fig. 5, we present branching ratios of the decay processes $t \rightarrow \chi_{cJ} + W^+ + b$ at the NLO as a function of the matrix element ratio r varying from 0.31 to 0.40. In these processes, the CO contributions are dominant at the LO. When we use the \overline{MS} subtraction scheme in renormalizing the NRQCD LDMEs $\langle \mathcal{O}^{\chi_{cJ}}[{}^3S_1^{(8)}] \rangle$ and set factorization scale $\mu_\Lambda = m_c$, the NLO CO give a big positive correction, and the $^3P_J^{(1)}$ Fock state gives a negative contribution. From our calculation, we can see that if the value of r favors the Tevatron data and CMS data, there will not be too much parameter space

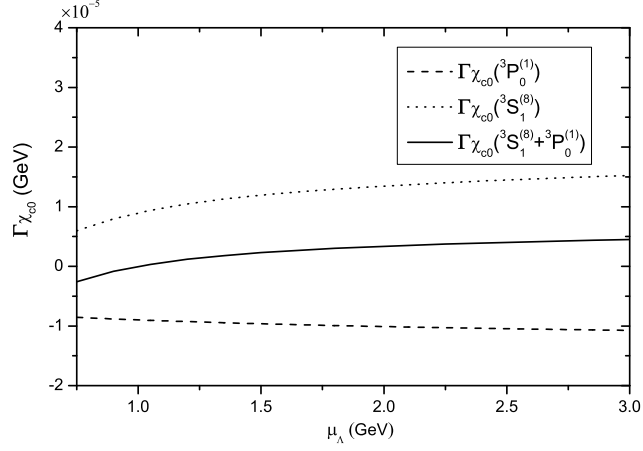


FIG. 4: The μ_Λ dependence of the χ_{c0} NLO total decay width, the $^3S_1^{(8)}$ - and $^3P_0^{(1)}$ -channel decay widths.

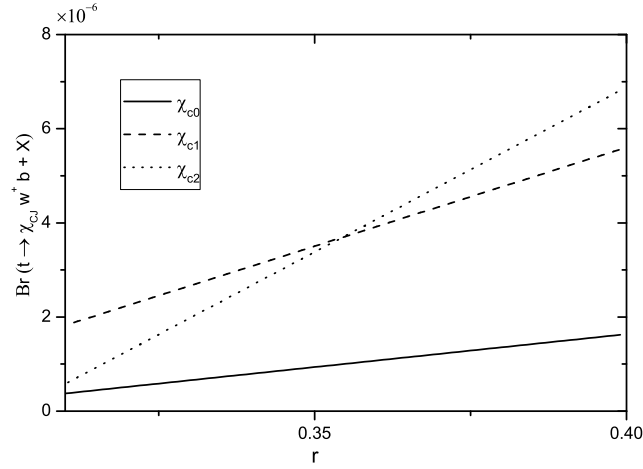


FIG. 5: Branching ratio of the decay processes $t \rightarrow \chi_{cJ} + W^+ + b$ at NLO as a function of the matrix element ratio r .

to accommodate it, the branching ratios of the decay processes $t \rightarrow \chi_{cJ} + W^+ + b$ are very small, and detecting these processes will not be easy. Meanwhile, the indirect prompt J/ψ production for the χ_{cJ} decay will be very small and negligible. If the value of r favors the LHCb data, detecting χ_{c0} production from top-quark decay is still very difficult, but χ_{c1} and χ_{c2} production may have the potential to be detected at the LHC, and the indirect prompt J/ψ production for the χ_{cJ} may not be so important as estimated by LO calculation.

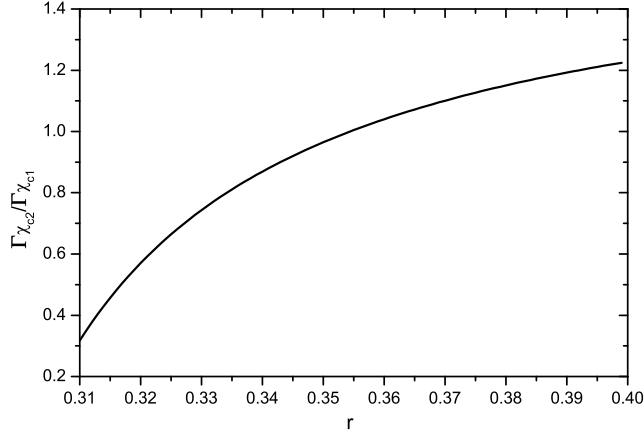


FIG. 6: The ratio $R_{\chi_c} = \frac{\Gamma_{\chi_{c2}}}{\Gamma_{\chi_{c1}}}$ at the NLO as a function of the the matrix element ratio r .

In Fig. 6, we also give the ratio $R_{\chi_c} = \frac{\Gamma_{\chi_{c2}}}{\Gamma_{\chi_{c1}}}$ at the NLO as a function of the matrix element ratio r and varying it from 0.31 to 0.40. If we only consider the LO contribution, we can get the ratio to be $5/3$ by spin counting easily. However, at the NLO, the ratio R_{χ_c} has been changed significantly for the $^3P_J^{(1)}$ -state contribution. When varying r from 0.31 to 0.40, the ratio R_{χ_c} can be changed from 0.31 to 1.22. With the growth of the value of r , the $^3P_J^{(1)}$ -state contribution will become less important, and the ratio R_{χ_c} will tend to be the spin counting result $5/3$.

IV. SUMMARY

In conclusion, we have considered the NLO QCD corrections for the excited charmonium production processes $t \rightarrow \chi_{cJ} + W^+ + b$ in top-quark decay. These processes are an interesting platform for studying the heavy quarkonium production mechanism. We adopt the dimensional regularization to deal with the UV and IR singularities in our calculation. The Coulomb singularities and soft singularities in P state are isolated and absorbed into the NRQCD NLO-corrected operator $\langle \mathcal{O}^{\chi_{cJ}}[{}^3S_1^{(8)}] \rangle$. After adding all contributing components together, we obtain the results with UV, IR, and Coulomb safety. In these processes, the CO contributions are dominant at the LO. When we use the \overline{MS} subtraction scheme in renormalizing the NRQCD LDMEs $\langle \mathcal{O}^{\chi_{cJ}}[{}^3S_1^{(8)}] \rangle$ and set factorization scale $\mu_\Lambda = m_c$, the NLO CO gives a big positive correction, and the $^3P_J^{(1)}$ Fock state gives a negative contri-

bution. From our calculation, detecting χ_{c0} production from top-quark decay may be very difficult, but χ_{c1} and χ_{c2} production may have the potential to be detected at the LHC. Detailed study of the prompt χ_{cJ} production from top-quark decay at the LHC is not only very useful for investigating J/ψ production from top-quark decay but is also important in understanding the heavy quarkonium production mechanism.

V. ACKNOWLEDGMENTS

This work was supported in part by the National Natural Science Foundation of China (Grants No.11305001, No.11205003, No.11535002, No.11375171, and No.11275190).

-
- [1] G.T. Bodwin, E. Braaten and G.P. Lepage, Phys. Rev. **D 51** (1995) 1125, erratum ibid. **D 55** (1997) 5853.
 - [2] Y.-Q. Ma, K. Wang, and K.-T. Chao, Phys. Rev. Lett. **106**, 042002 (2011) [arXiv:1009.3655 [hep-ph]].
 - [3] M. Butenschön and B. A. Kniehl, Phys. Rev. Lett. **106**, 022003 (2011) [arXiv:1009.5662 [hep-ph]].
 - [4] B. Gong, L.-P. Wan, J.-X. Wang, and H.-F. Zhang, Phys. Rev. Lett. **110**, 042002 (2013) [arXiv:1205.6682 [hep-ph]].
 - [5] M. Butenschön and B. A. Kniehl, Phys. Rev. Lett. **104**, 072001 (2010) [arXiv:0909.2798 [hep-ph]].
 - [6] M. Butenschoen and B. A. Kniehl, Phys. Rev. Lett. **107**, 232001 (2011) [arXiv:1109.1476 [hep-ph]].
 - [7] Y.-Q. Ma, K. Wang, and K.-T. Chao, Phys. Rev. D **83**, 111503(R) (2011) [arXiv:1002.3987 [hep-ph]].
 - [8] M. Butenschoen and B. A. Kniehl, Phys. Rev. Lett. **108**, 172002 (2012) [arXiv:1201.1872 [hep-ph]].
 - [9] K.-T. Chao, Y.-Q. Ma, H.-S. Shao, K. Wang, and Y.-J. Zhang, Phys. Rev. Lett. **108**, 242004 (2012) [arXiv:1201.2675 [hep-ph]].

- [10] H.-S. Shao, Y.-Q. Ma, K. Wang, and K.-T. Chao, Phys. Rev. Lett. **112**, 182003 (2014) [arXiv:1402.2913 [hep-ph]].
- [11] H.-S. Shao, H. Han, Y.-Q. Ma, C. Meng, Y.-J. Zhang, and K.-T. Chao, J. High Energy Phys. **05** (2015) 103 [arXiv:1411.3300 [hep-ph]].
- [12] M. Klasen, B. A. Kniehl, L. N. Mihaila, and M. Steinhauser, Nucl. Phys. **B713**, 487 (2005) [hep-ph/0407014].
- [13] M. Klasen, B. A. Kniehl, L. N. Mihaila, and M. Steinhauser, Phys. Rev. D **71**, 014016 (2005) [hep-ph/0408280].
- [14] M. Butenschoen and B. A. Kniehl, Phys. Rev. D **84**, 051501(R) (2011) [arXiv:1105.0820 [hep-ph]].
- [15] Zhi-Guo He, Ying Fan and Kuang-Ta Chao, Phys. Rev. Lett. **101**, 112001 (2008) [arXiv:0802.1849].
- [16] Ying Fan, Zhi-Guo He, Yan-Qing Ma and Kuang-Ta Chao, Phys. Rev. **D 80**, 014001 (2009) [arXiv:0903.4572].
- [17] E. Braaten and S. Fleming, Phys. Rev. Lett. **74**, 3327 (1995) [hep-ph/9411365].
- [18] Kuang-Ta Chao, Yan-Qing Ma, Hua-Sheng Shao, Kai Wang, and Yu-Jie Zhang, Phys. Rev. Lett. **106**, 042002 (2011) [arXiv:1201.2675] .
- [19] B. Gong, L.-P. Wan, J.-X. Wang, and H.-F. Zhang, (2013), arXiv:1305.0748; CDF, A. A. Affolder *et al.*, Phys. Rev. Lett. **85**, 2886 (2000), arXiv:hep-ex/0004027; CMS Collaboration, S. Chatrchyan *et al.*, Phys.Rev.Lett. **110**, 081802 (2013), arXiv:1209.2922; (2014), arXiv:1410.8537.
- [20] Z. G. He and B. A. Kniehl, Phys. Rev. D **92**, 014009 (2015) [arXiv:1507.03883 [hep-ph]].
- [21] U. Langenfeld, S. Moch and P. Uwer, arXiv:0907.2527 [hep-ph].
- [22] N. Kidonakis and R. Vogt, Phys. Rev. D **78**, 074005 (2008) [arXiv:0805.3844 [hep-ph]].
- [23] Q. L. Liao, X. G. Wu, J. Jiang, G. Chen and Z. Y. Fang, arXiv:1304.1303 [hep-ph].
- [24] C. F. Qiao, C. S. Li and K. T. Chao, Phys. Rev. D **54**, 5606 (1996) [hep-ph/9603275].
- [25] Cong-feng Qiao, Kuang-Ta Chao, Phy. Rev. **D 55**, 2837 (1997) [arXiv:9606462].
- [26] F. Yuan, C. F. Qiao and K. T. Chao, Phys. Rev. D **57**, 610 (1998) [hep-ph/9709400].
- [27] P. Sun, L. P. Sun and C. F. Qiao, Phys. Rev. D **81**, 114035 (2010) [arXiv:1003.5360 [hep-ph]].
- [28] Song Mao, Li Gang, Zhou Ya-Jin, Guo Jian-You, and Ma Zheng-Wei, Phys. Rev. D **91**, 116004 (2015).

- [29] A. Petrelli, M. Cacciari, M. Greco, F. Maltoni and M. L. Mangano, Nucl. Phys. B **514**, 245 (1998) [hep-ph/9707223].
- [30] M. Kramer, Nucl. Phys. B **459**, 3 (1996).
- [31] W. T. Giele and E. W. N. Glover, Phys. Rev. **D46** (1992) 1980; W. T. Giele, E. W. Glover and D. A. Kosower, Nucl. Phys. B **403** (1993) 633; S. Keller and E. Laenen, Phys. Rev. **D59** (1999) 114004.
- [32] E.J. Eichten and C. Quigg, Phys. Rev. **D52**, 1726 (1995).